PRODUCTION TECHNOLOGIES FOR EXPLOITATION OF GAS HYDRATES

By

A.NAGESH

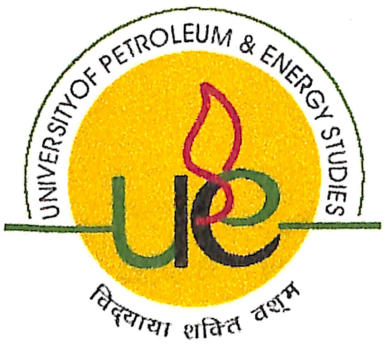

College of Engineering
University Of petroleum and Energy Studies
Dehradun
May-2008

PRODUCTION TECHNOLOGIES FOR EXPLOITATION OF GAS HYDRATES

A thesis Submitted in partial fulfillment of the requirement for the degree of
Master of Technology
Gas Engineering

By
A.Nagesh

Under the guidance of

Mr.S.Sahai
Adjunct Professor

Approved

Dr.B.P. Pandey
Dean

College Of Engineering
University Of petroleum and Energy Studies
Dehradun
May-2008

CERTIFICATE

This is to certify that the work contained in this thesis titled "Production Technologies for Exploitation of Gas Hydrates" has been carried out by A.Nagesh under my/our supervision and has not been submitted elsewhere for a degree.

Mr.S.Sahai
Adjunct Professor
College of Engineering
UPES

Date:

porate Office:
lrocarbons Education & Research Society
Floor, PHD House,
Siri Institutional Area
just Kranti Marg, New Delhi - 110 016 India
+91-11-41730151-53 Fax : +91-11-41730154

Main Campus:
Energy Acres,
PO Bidholi Via Prem Nagar,
Dehradun - 248 007 (Uttarakhand), India
Ph.: +91-135-2102690-91, 2694201/ 203/ 208
Fax: +91-135-2694204

Regional Centre (NCR) :
SCO, 9-12, Sector-14,
Gurgaon 122 007
(Haryana), India.
Ph: +91-124-4540 300
Fax: +91-124-4540 330

Regional Centre (Rajahmundry):
GIET, NH 5, Velugubanda,
Rajahmundry - 533 294,
East Godavari Dist., (Andhra Pradesh), India
Tel: +91-883-2484811/ 855
Fax: +91-883-2484822

Email: info@upes.ac.in URL: www.upes.ac.in

ABSTRACT

Methane hydrate presents a potentially enormous amount of energy assuming technology can be developed for commercial production. The aim of the project is to examine the feasibility of recovery of gas hydrates from Hydrate Ridge. In the present analysis, reservoir assessment of the hydrates, their recovery methods, their efficient utilization are considered. The initial estimate indicates that recovery of gas hydrate from the Hydrate Ridge is currently uneconomical. In the present case, due to the very small volume of gas the reservoir, injection of hot brine as a recovery method and depressurization technique is useful for large volume of reserves.

Keywords: hydrate recovery, depressurization.

ACKNOWLEDGEMENT

This is to acknowledge with thanks the help, guidance and the support that I have received during the project work.

I wish to express my appreciation and cordial thanks to **Prof. S. SAHAI**, Adjunct Professor, College of Engineering, UPES, Dehradun and **Dr. B. P. PANDEY**, Dean, College of Engineering, UPES and **Dr. D. N. SARAF,** Distinguised Professor, College of Engineering, UPES for making provisions and encouraging me for my major project, which has been of inestimable value in my pursuit of achieving the Masters in Gas Engineering from University of Petroleum and Energy Studies.

I am especially grateful to **Dr R. P. BADONI,** (Course Coordinator, M.Tech (Gas Engineering)) for his encouragement, valuable remarks and comments during the entire project.

I avail this opportunity to place my profound sense of gratitude to my project guide **Prof. S. SAHAI** Adjunct Professor of College of Engineering, UPES, Dehradun. I am very grateful to him for his support, guidance, assistance, patience and enthusiasm

I am immensely indebted to my parents, who have always rendered their support and helped me to complete this project successfully. Last but not least thanks to my friends and colleagues who helped me in making numerous improvements not only to its wording but to its technical content.

A.NAGESH

R030206001

M. Tech (Gas Engineering)

U.P.E.S, Dehradun

Email ID: nagesh.mtech@gmail.co

CONTENTS

LIST OF FIGURES

LIST OF PLOTS

LIST OF TABLES

NOMENCLATURE

C_p	Heat capacity (J/K kg)
$m^{\cdot}$	Mass flow rate
n_H	Mole of methane gas
ΔG	Gibb's Free Energy
ΔH	Enthalpy of hydrate dissociation
Φ_H	Volume fraction of hydrate in the core
φ	Porosity
Ψ	dimensionless surface roughness factor
ρ	Density of the porous medium including the hydrate (kg/m^3)
μ_g	Viscosity of gas (cp)
ρ_H	Density of the pure methane hydrate (kg/m^3)
ρ_R	Density of the porous medium (kg/m^3)
μ_w	Viscosity of water (cp)
ρ_W	Density of pure water (kg/m^3)
a_{dec}	Specific decomposing hydrate surface area per unit hydrate volume
a_{geo}	Geometry surface area
$\Delta E/R$	Activation energy over the gas constant (K)
f_g	Fugacity of methane at the solid surface
F	Faraday's constant
F_{Hg}	Mass fraction of gas in unit mass of hydrate ($KgCH_4/KgHydrate$)
f_{se}	Fugacity of methane at the three-phase equilibrium pressure
k	Phase permeability (mD)
k	Thermal conductivity of hydrate (kW/m^2 K)
k_0	Intrinsic rate constant for decomposition ($kmol/m^2$-kPa-s)
k_d	Decomposition rate constant ($kmol/m^2$-kPa-s)

k_{gw}	Relative permeability with respect to gas
k_{rw}	Relative permeability with respect to water
MW_H	Molecular weight of hydrate (g/mol CH_4 in hydrate)
p_1	Initial pressure (MPa)
p_2	Formation pressure (MPa)
p_g	Pressure of methane at the solid surface
p_G	Pressure at the well (MPa)
p_i	Initial pressure (MPa)
p_o	Wellbore pressure (MPa)
p_{se}	Equilibrium pressure at the dissociation interface temperature (MPa)
P	Power (W)
Q	Heat defined as mcpΔT
q_s	Specified heat flux at the decomposing surface (k W/m^2)
Ste	Stefan number
t	Time
T_1	Initial gas temperature (K)
T_2	Final gas temperature (K)
T_i	Initial temperature (K)
T_{oc},	Equilibrium temperature at the wellbore pressure (K)
T_s	Temperature of the dissociation interface (K)
$X(t)$	Position of the dissociation interface as a function of time (m)
ΔT	Temperature difference between the bulk fluid and the hydrate interface
η_c	Efficiency of the compressor
λ	Solution of eq. 5.3

CHAPTER 1

1.1 INTRODUCTION:

Some compounds crystallize in such a way that a hole is formed inside the crystal which can accommodate another guest molecule without forming any chemical bond. There complexes are known as inclusion or clathrate compounds. The inclusion of the guest molecule depends on the steric fit inside the crystal lattice and is often very selective.[1]

In host-guest chemistry an inclusion is a complex in which one chemical compound the host forms a cavity which molecule of a second compound the guest are located. The definition of inclusion compounds is very broad it extends to channels formed between molecules in a crystal lattice in which guest molecules can fit. If spaces in the host lattice are enclosed on all sides so that the guest species is 'trapped' as in a cage, such compounds are known as clathrate. The word clathrate is derived from the Latin clatratus meaning with bars or a lattice. In molecular encapsulation a guest molecule is actually trapped inside another molecule. In supramolecular chemistry, host-guest chemistry describes complexes that are composed of two – or more molecules or ions held together in unique structural relationship by hydrogen bonding or by ion pairing or by vanderwaals force other than those of full covalent bonds. Clathrate compounds constitute relatively small segments of that group of complexes molecules which has been designated as molecular compounds.

In 1945, H.M.Powell named these compounds clathrate. Clathrate complex used to refer only to the inclusion complex of hydroquinone, but recently it has been adopted for many complexes which consist of host molecule (forming the basic frame) and guest molecule (set in the host molecule by interaction). The clathrate complexes are various and include, for e.g., strong interaction via chemical bond between host molecules and guest molecules, or guest molecules set in the geometrical space of host molecules by weak intermolecular force. Typical examples of host- guest complexes are inclusion compounds and intercalation compounds. Clathrates were studied by P.Pfeiffer in 1927[2] and in 1930. One of the early attempts to describe these molecular compounds was that of Hertal who wrote, "a molecular compound is a substance formed from to different compounds each of which may have an independent crystal structure and which in solution (or the vapor state), and decomposes in its components according to the law of mass action.

The force which holds them together in the molecular compound has been called secondary valence or residual affinity. Today this is neither complete or a satisfactory description of molecular compounds, though it reference an attempt to provide some basis in which lines of demarcation between complex compounds may be drawn. Based on this Clapp presented a organic molecular compounds which further organized the field. He divided them in to four groups.

Clapp's classification[4]:

1. The products formed from Benzoquinone, substituted quinine, or closely related compounds with aromatic hydrocarbons, amines, phenols, and aromatic ethers.
2. The products of nitro compounds with aromatic hydrocarbons, halides, amines and phenols.
3. The compounds formed by the bile salts with fatty acids, ester, paraffins and few other compounds.
4. The compounds containing a hydrogen bond.

Clapp also pointed out some properties which organic molecular compounds have in common such as,

i. The ease with which many of them may be prepared, their tendency to decompose rather than melt, and their dissociation in their components when put in to solution.

ii. Polarization is readily recognized as a property which can bring about the formation of molecular compounds; however the polarization of aggregates caused by the electrostatic attraction does account for simple molecular ratios in the compounds formed

iii. Molecules of marked size differences are expected to react with molecule of second components to give molecular compounds in which the ratios of two components are the same, because the electron field about the components cannot, of course, be uniform. However, surprisingly, the ratios observed between the two components are largely whole number ratios.

A group known as occlusion compounds, or inclusion compounds, is found in Clapp's third class of organic molecular compounds. This third class is composed of organic molecular compounds in which the chemical properties of the components are subordinate to the sizes and geometrics of the molecules; the stereochemistry and size relationships of inclusion compounds play major roles in the behavior. Because the utility of inclusion process has been only recently recognized, the unique characteristics of inclusion compounds have had limited application in industry and research.

When writing of molecular compounds, Ketelaar refers to the vanderwaals forces which are actually one-tenth to one-twentieth has large as the energy of most atomic or ionic bonds; consequently they do not give rise to the formation of chemical compounds with stable molecules. Compounds in which bonding by vanderwaal's forces includes numerous so called "molecular compounds". Ketelaar divides them as follows[5]:

Ketelaar Classification:

1. Molecular compounds which have formed have a result of the favorable mutual orientation of their two components, each of which possesses a dipole, and include:
    a. Clathrates
    b. Gas hydrates
    c. Urea adducts
2. Molecular compounds which are formed by the exchange of atoms and include:
    a. Those in which the free electron pair of the donor and the incomplete electron configuration of the acceptor are already present.
    b. Those in which they are not.

In still another account of molecular compounds, that of Robertson[6], attention is called to the fact that, though hydrogen bonding is perhaps the most universal certainly the most studied form of molecular association, their does exists a unique group of molecular compounds in which hydrogen bonding place a minor role, or is even non existent. Excluding all molecular compounds in which hydrogen bonding may be exclusively responsible for bonding involved, four cases are cited:

(a) Molecular compounds formed between aromatic hydrocarbons and poly nitro Compounds.

(b) Addition compounds formed by polycyclic hydro carbons with certain halogens or with antimony Penta chloride.

(c) Loose addition complexes formed between unsaturated compounds and copper, silver or mercury salts.

(d). Clathrates

Baron Classification:

Baron[7] has listed these divisions as:

1) Poly molecular inclusion compounds

   (a). Those with channel – Like spaces

   (b). Those with cage – Like spaces

2). Mono molecular inclusion compounds

3). Macro molecular inclusion compounds

4). Products of the blue iodine reaction.

An essential characteristic of the host is its ability to form a solid structure with hollow spaces of large enough dimensions to house prospective guests. The inclusion compound which forms will have a stability largely attributed to the way in which the molecules involved fit together in space. When inclusion occurs, the host and guest molecules must be properly oriented with respect to one another, under optimum conditions for formation. Wheland[14] illustrated this with a simplified two dimensional analog, using small irregular closed curves (B) to represent the guest molecules and similarly larger irregular closed curves (A) to represent the host structure.

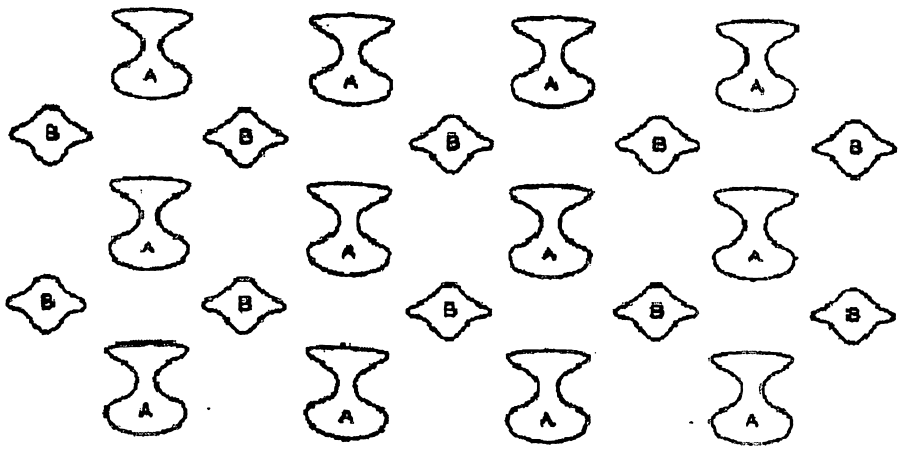

Figure 1.1 A schematic two-dimensional representation of a small region within an inclusion compound that is formed from molecules of a trapping component, A, and of a trapped component, B.

In mono molecular inclusion compounds, only one molecule is host to a guest molecule. Obviously the host molecule will be large and will have a cage like space in its centre. Typical of mono molecular inclusion compounds are the cyclodextrins.

Macro molecular inclusion, some of which have been described as "molecular sieves". The zeolites, among the best known, are inclusion compounds whose inclusion properties have found wide industrial application. Essentially they are crystalline structures in which a frame works of silicon-oxygen or oxygen-aluminum tetrahedral form the basic structure. This crystalline to provide a 3-D network which is permitted with relatively large channels and cavities. These interstices normally enclose water molecules which are removed quite easily, simply by heating the compound the holes which are left by the evacuated water molecules can be filled with amazing nos. of gas, vapors or dissolved compound molecules. Curiously, of all the host lattices compared here, the zeolites are the only ones stable in the absence of guest molecules and which permit migration of suitable small guest molecules from one cavity to another throughout the crystal.

1.2 Natural gas Hydrates

Natural gas hydrates are solid crystalline compounds, which have a structure wherein guest molecules are entrapped in a cage like framework of the host molecules without forming a chemical bond. It is a result of the hydrogen bond that water can form hydrates.

The hydrogen bond causes the water molecules to align in regular orientations. The presence of certain compounds causes the aligned molecules to stabilize, and a solid mixture precipitates. The water molecules are referred to as the host molecules, and the other compounds, which stabilize the crystal, are called the guest molecules. The hydrate crystals have complex, three dimensional structures in which the water molecules form a cage and the guest molecules are entrapped in the cages.

The stabilization resulting from the guest molecule is postulated to be caused by Vander Waals forces, which is the attraction between molecules that is not a result of electrostatic attraction. The hydrogen bond is different from the Vanderwaal's force because it is due to strong electrostatic attraction, although some classify the hydrogen bond as a Vander walls force. Another interesting thing about gas hydrates is that no bonding exits between the guest and host molecules. The guest molecules are free to rotate inside the cages built up from the host molecules. This rotation has been measured by spectroscopic means. No hydrate with out guest molecules has been found in nature. Thus Clathrates are stabilized by the weak attractive interactions between guest and water molecules. However, the guest species has some restrictions on its size. This arises from the fact that there are a limited no. of cage types which encapsulate guest molecule with out deviation of the hydrogen bond lengths and angle from ideal ones. All of the cages are not necessarily depends on the temperature and the pressure of the guest compound in equilibrium with clathrate hydrate.

1.3 Structures of Gas Hydrates

- S I structure
- S II structure
- H structure

S I STRUCTURE

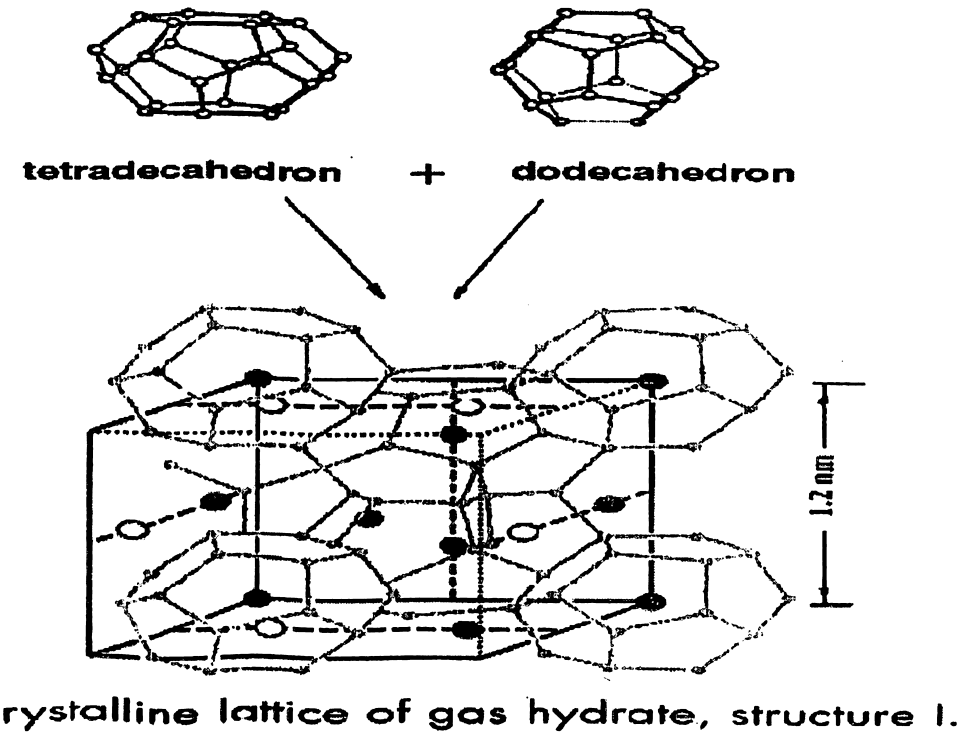

Figure 1.2 Structure I Hydrate

S II STRUCTURE

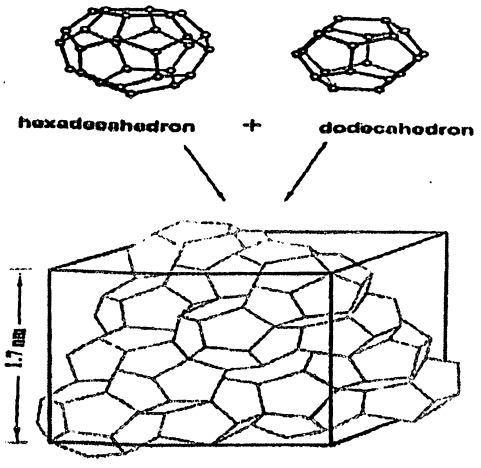

Crystalline lattice of gas hydrate, structure II

Top View of the Structure H Hydrate Unit Cell

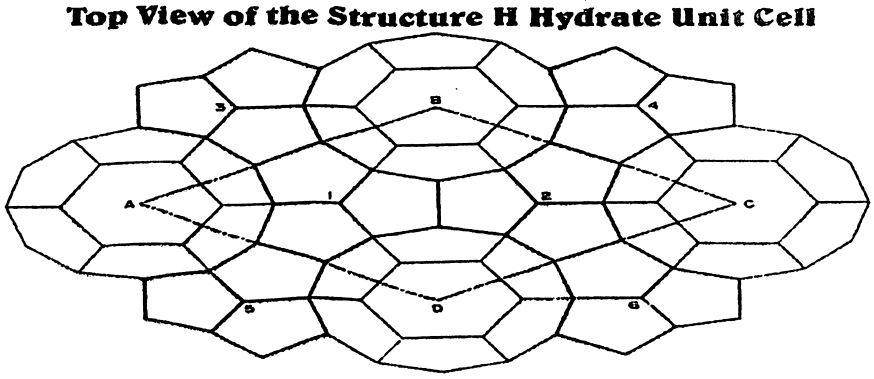

Side View of the Structure H Hydrate Unit Cell

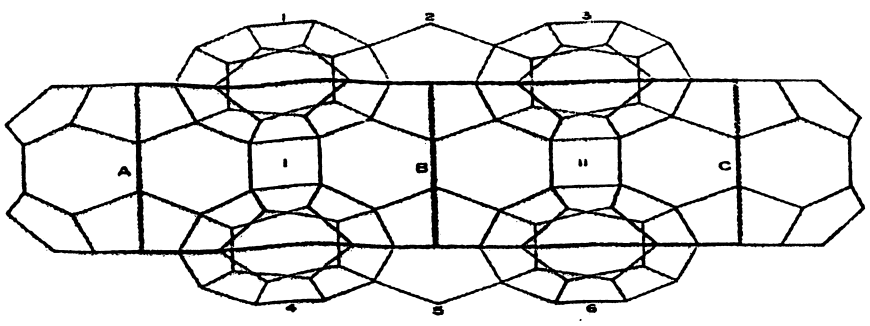

Figure 1.3 Structure II and Structure H Hydrate

Parameter	*Structure I*	*Structure II*
Cage size, nm	1.203	1.731
Number of dodecahedra	2	16
Number of tetradecahedra	6	–
Number of hexadecahedra	–	8
Coordination number (number of water molecules in a single cage)		
in a small cage	20	20
in a large cage	24	28
Number of water molecules in the unit cell	46	136
Number of cages		
large	6	8
small	2	16
Cage diameter, nm:		
large	0.86	0.946
small	0.788	0.782
Ideal composition*	$6G{\cdot}2M{\cdot}46H_2O$	$8G{\cdot}16M{\cdot}136H_2O$

*Ideal composition of hydrate is obtained when all large cages are filled with the G molecules and small cages with the M molecules.

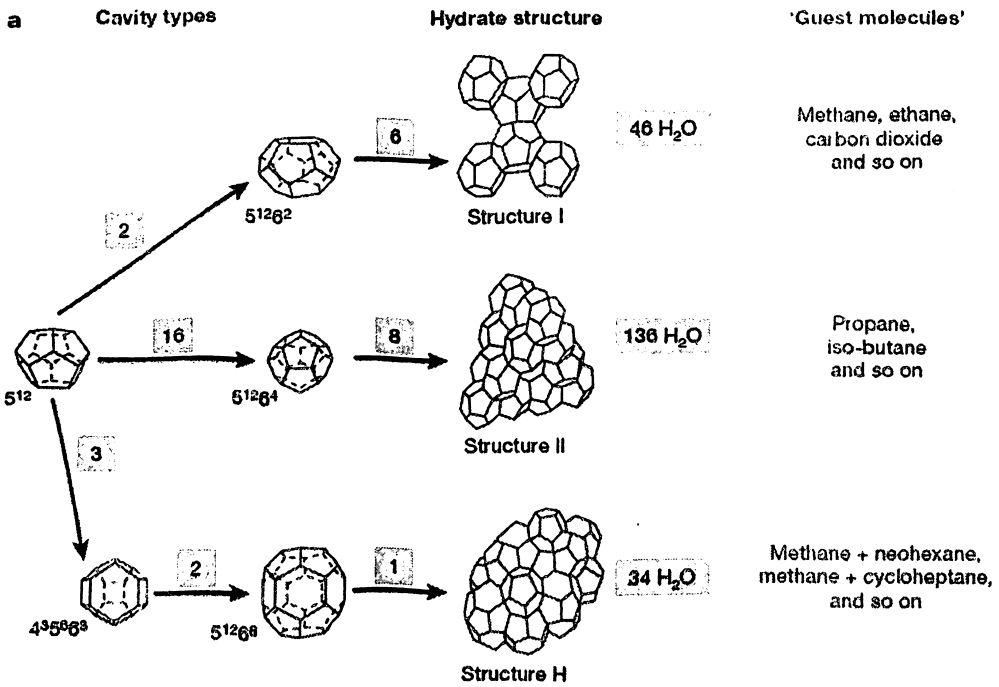

b

Hydrate crystal structure	I		II		H		
Cavity	Small	Large	Small	Large	Small	Medium	Large
Description	5^{12}	$5^{12}6^2$	5^{12}	$5^{12}6^4$	5^{12}	$4^35^66^3$	$5^{12}6^8$
Number of cavities per unit cell	2	6	16	8	3	2	1
Average cavity radius (Å)	3.95	4.33	3.91	4.73	3.91†	4.06†	5.71†
Coordination number*	20	24	20	28	20	20	36
Number of waters per unit cell	46		136		34		

*Number of oxygens at the periphery of each cavity.
†Estimates of structure H cavities from geometric models.

**The three common hydrate unit crystal structures. [14]

Figure 1.4 The three common hydrate unit crystal structures.

Note:

Nomenclature: 5^{12} 6^4indicates a water cage composed of 12 pentagonal and four hexagonal faces. The numbers in squares indicate the number of cage types. For e.g. The Structure I unit crystal is composed of two 5^{12} cages, six $5^{12}6^4$ cages and 46 water molecules.

STRUCTURE I:

Structure I gas hydrates are formed when there cavities arrange themselves in space in a manner that they link together through their vertices. Because dodecahedra are not able to pack together precisely, a tetrakai decahedron, a polyhedron with 12 pentagonal and 2 hexagonal faces, is created. Oxygen atoms of these water molecules are arranged in such a

manner that two pentagonal dodecahedra and six tetrakai decahedra are formed. It has a cubic cell constant of 12^0A and forty six molecules of water constitute the unit cell, two of which are small and contain only one small guest molecule. The other six cavities can house relatively larger molecule.

They are Simple structure, made from two types of cages.

- Dodecahedron, a 12 sided polyhedron where each face is pentagon.
- Tetrakaidcahedron a 14 sided polyhedron with 12 pentagonal faces and 2 hexagonal faces.
- Dodecahedron cages are smaller than the tetrakaidecahedron cages.
- Stable hydrate can form with out a guest molecule occupying all the cages. The degree of saturation is a function of temperature and pressure. Actual composition of hydrate is not the theoretical composition.

The theoretical formula for hydrate is $X \cdot 5¾H_2O$, where X is the hydrate former. If the guest molecule occupies only large cages, then the formula for hydrate is $X \cdot 7\ 2/3\ H_2O$.

STRUCTURE II:

Structure II gas hydrates are formed when the pentagonal dodecahedron cavities arrange themselves in space in a manner that they link together through face sharing. As a result of this arrangement, hexakai dodecahedron, a polyhedron with 12 pentagonal and 4 hexagonal faces, is created. It has a cubic cell constant of 17^0A; one hundred and thirty six water molecules are associated in each cell. These form sixteen small and eight relatively large cavities.

It also construct from two types of cages.

- Dodecahedron, a 12 sided polyhedron where each face is regular pentagon.
- Hexkaidcahedron a 16 sided polyhedron with 12 pentagonal faces and 4 hexagonal faces. Dodecahedron cages are smaller than the tetrakaidecahedron cages.

It contains 136 water molecules. If the guest molecule occupies all the cages, then the theoretical formula for hydrate is $X \cdot 5\frac{2}{3}H_2O$, where X is the hydrate former. If the guest molecule occupies only large cages, then the theoretical composition is $X \cdot 17H_2O$.

STRUCTURE H:

This is much less common than either S I & S II. In order to form, this type of hydrate requires small molecules such as methane and type H former. This type hydrate constructed some three types of cages.

- Dodecahedron, a 12 sided polyhedron where each face is regular pentagon.
- An irregular dodecahedron with three square faces 6 pentagonal faces and three hexagonal faces.
- An irregular icosohedron a 20 sided polyhedron with 12 pentagonal faces and 8 hexagonal faces.

It contains 34 water molecules the theoretical formula is $(Y)(5X)(34H_2O)$

Where,

X=small molecule, enters only to small cages.

Y=large molecule enters only to large cages

Structure H in which the largest cage can accommodate up to 5 argon atoms.

H Forming Molecule:

2 methyl butane, 2-2 dimethyl butane, 2-3 dimethyl butane, 2-2-3 tri methyl butane, 3-3 di methyl pentane, methyl cyclopentane, ethylcyclo pentane, methyl cyclohexane, cycloheptane and cyclo octane.

CHAPTER 2

2.1 GLOBAL POTENTIAL OF GAS HYDRATES

At present, approximately 50 locations worldwide have been identified where geophysical and geochemical evidence indicates the occurrence of natural gas hydrates (Kelland, 1994). Quantification of the amount of gas, mostly methane, stored in hydrates reservoirs is difficult since only a few of the sites have been drilled and tested for their hydrates content. Estimates of the methane content of these reservoirs obtained by several researchers are summarized in Table (Kelland, 1994). Gas hydrates in oceanic sediments may comprise the earth's largest fossil fuel reservoir.

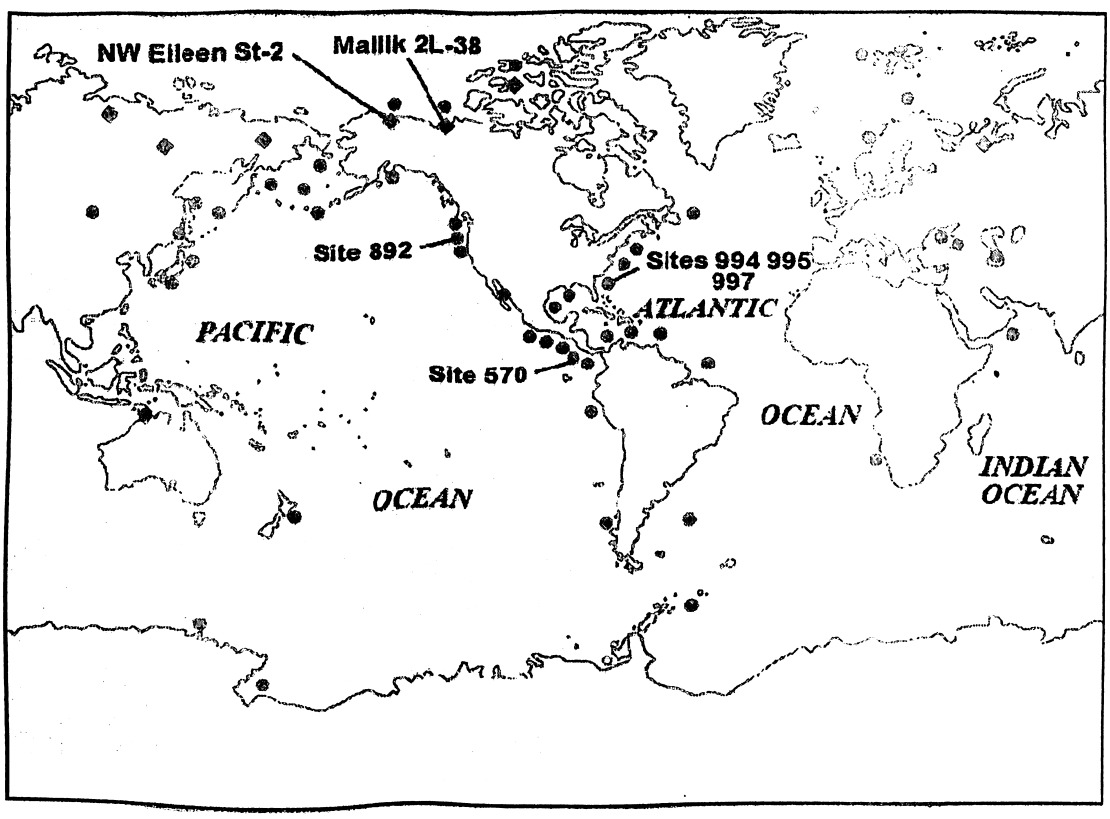

Source: U. S. Geological Survey, Denver Federal Center, Box 25046, MS-939, Denver, Colorado, 80225;

Figure 2.1: Locations of known and inferred gas hydrate occurrences in oceanic sediment of outer continental margins (circles) and permafrost regions (diamonds) (modified from Kvenvolden, 1993).

Table 2.1: The Earth's Organic Carbon Endowment by Location (Reservoir)

Reservoir	Organic Carbon	
	10^{13} Kilograms	Trillion Short Tons
Gas Hydrates (on- and offshore)	10,000	110,230
Fossil Fuels (coal, oil, natural gas)	5,000	55,116
Soil	1,400	15,432
Dissolved Organic Matter in Water	980	10,803
Land Biota	830	9,149
Peat	830	9,149
Detrital Organic Matter	60	661
Atmosphere	3.6	40
Marine Biota	3	33

Note: As a point of reference, the Great Lakes' 5,500 cubic miles of fresh water have a mass of about 25.2 trillion short tons.

Source: K.A. Kvenvolden, "Gas hydrates - geologic perspective and global change," Review of Geophysics 31 (1993), pp. 173-187.

TABLE 2.2: GAS AND GAS HYDRATES RESERVES (FROM KELLAND, 1994)

In-situ gas hydrates estimate range	
Onshore, continental	$14 - 34\,000 \times 10^{12}\ m^3$
Offshore, oceanic	$3100 - 7\,600\,000 \times 10^{12}\ m^3$
Unexploited conventional gas reserves	$260 \times 1012\ m^3$

2.2 INDIAN POTENTIAL OF GAS HYDRATES

National Gas Hydrate Programme (NGHP) has brought out highly prospective hydrate deposits in the offshore region of Kutch, Saurashtra, Mumbai, Kochi, Konkan, Trivandrum, Cauvery basin, Krishna Godavari, Andaman Nicobar and Gulf of Mayan mar with total estimated hydrate resources of 1894 TCM.

The amount of natural gas stored in natural gas hydrates is estimated at about 20,000 TCM, a figure nearly two order of magnitudes larger than recoverable conventional gas resources. Hence, gas hydrates provide an energy supply assurance for the 21st century. Another important factor is that methane is a less carbon-intensive fuel than coal or oil. Methane from hydrates (or other sources) produces only half as much carbon dioxide as coal per unit of combustion products. Two thirds of coal combustion products are CO_2 vs. one third of methane[8].

$$2 \text{ coal (CH)} + 2\ ½\ O_2 \rightarrow 2\ CO_2 + H_2O$$

$$CH_4 + 2\ O_2 \rightarrow CO_2 + 2\ H_2O$$

Therefore, the utilization of the methane contained in natural gas hydrate would not only ensure the adequacy of world energy resources, but would also mitigate potential global climate change.

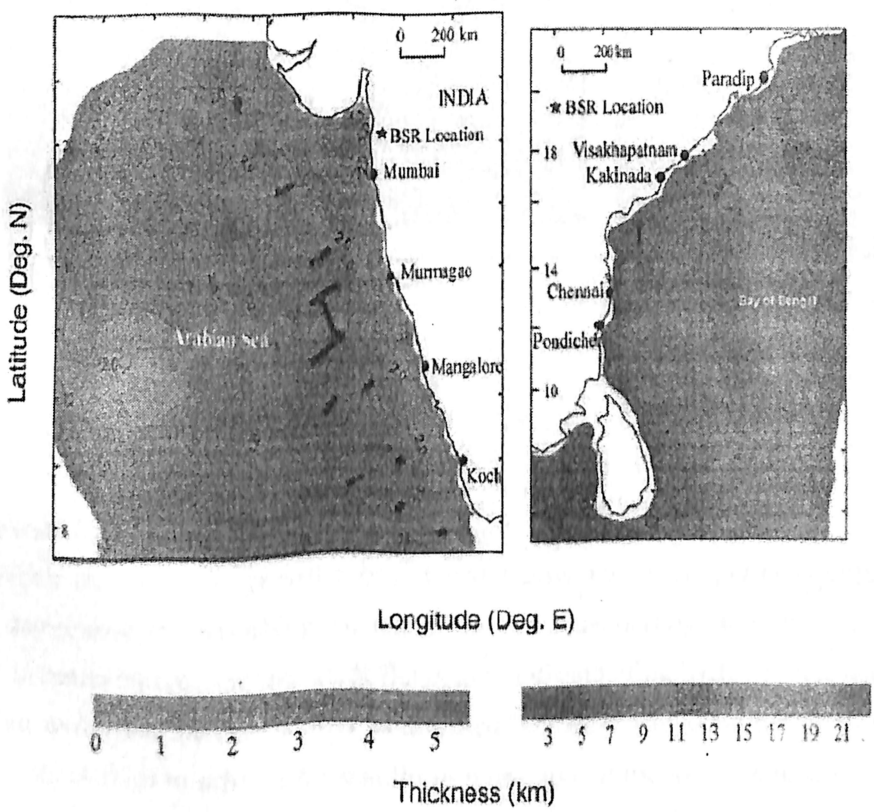

Figure 2.2: BSR locations on the sediment thickness map in western (left) and eastern (right offshore of India (Gupta et al., 1998).

Source: Department of Ocean Development, Government of India

CHAPTER 3

3.0 PRODUCTION METHODS OF GAS HYDRATES

Methane can be recovered from gas hydrates through modification of equilibrium conditions. Three common recovery methods employed are depressurization, inhibitor injection and thermal stimulation. The recovery method should be chosen on the basis of environmental damage as well as economics.

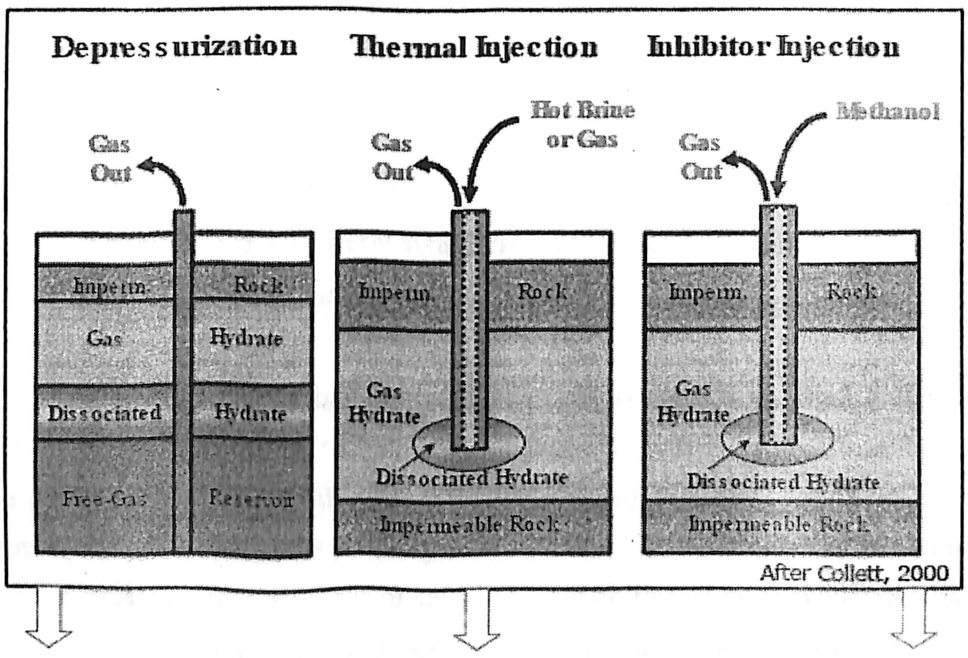

Figure 3.1 various production methods for gas hydrate.

3.1 Depressurization

When the reservoir pressure is reduced below the three phase equilibrium value, hydrate dissociates by absorbing energy from the surrounding and, hence, results in a decrease in reservoir temperature. Heat flows to the dissociating hydrate interface by thermal conduction and a thermal gradient is established. Hydrate will continue to dissociate until sufficient gas evolves to achieve the equilibrium pressure at the lower temperature. A thermal gradient has to be maintained in order to continue dissociation of the hydrate.

Among all three hydrate recovery methods, the depressurization is the most energy intensive method since there is no supply of energy or any chemical into the reservoir. Chemical reaction of methane with water to from hydrate is represented by

(CH4) gas + 6(H2O) water ↔ (CH4 • 6H2O) solid.

Three main mechanisms are involved in the depressurization of gas hydrates: fluid flow, heat transfer and kinetics. Many authors have been developing either analytical or numerical models to simulate the gas production from hydrate decomposition in porous media. The association process of these models was assumed to occur at a dissociation interface, which separates the reservoir into two zones: the gas zone near the well and the hydrate zone far away from the well. The dissociation interface moves forward into the reservoir with time. **Table 3.1** briefly summarizes the features of some models in terms of mechanisms and mathematical methods used.

In this work, a simple one-dimensional model is considered Fig.3.2. It should be noted that this wellbore model is linear, not radial. The effect of heat transfer, intrinsic hydrate decomposition, and fluids flow are calculated independently, i.e. if considered one mechanism, the other two effects are ignored, in order to determine the rate-controlling mechanism(s). An analytical model of methane hydrate decomposition for each of above three-mechanism is presented for a semi-infinite hydrate. The physical, chemical and geological parameters from the Hydrate Ridge Leg Nag-01 are used to simulate the effect of the three mechanisms mentioned above.

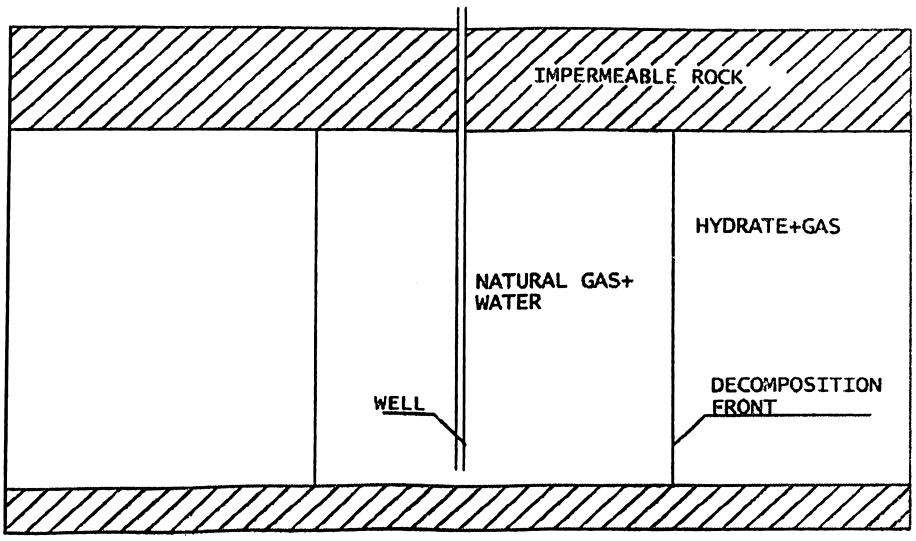

Figure 3.2 Schematics of the hydrate reservoir for the one-dimensional model.

Assume that there is a methane hydrate reservoir with initial pressure P_i and initial temperature T_i containing stable solid hydrate. When a well is drilled, the pressure drops to the wellbore pressure P_o below the pressure-temperature equilibrium condition. The hydrate in the neighborhood of the well starts to dissociate. The dissociation process is assumed to occur only at the front of the gas and hydrate zones instead of the entire volume. At $x=\infty$, it is assumed that the reservoir pressure and temperature are fixed at P_i and T_i, respectively. The dissociation interface, X (t), separates the reservoir into two zones. The area $0<x<X$ (t) is referred to as the gas zone and the area $X(t) <x<\infty$ is the hydrate zone. The dissociation interface moves outward as the gas production from the well continues.

In this work, the three phase equilibrium pressure-temperature is given by [Hong et al., 2003]:

$$P_{se} = 10^{-6} \exp(49.3185 - 9459/T_s) \qquad \text{– Equation 3.1}$$

Where T_s is in K and p_{se} is in *MPa*. p_{se} is the equilibrium pressure at the dissociation interface.

3.1.1 Decomposition Rate Controlled by Heat Transfer

To obtain the rate of decomposition by heat transfer, the effects of kinetics and fluids flow are ignored. The surrounding gas at the interface is at the thermodynamic equilibrium condition. The interface temperature is at T_{oe}, the equilibrium temperature at the wellbore pressure (p_o). Hence, the driving force for the heat transfer mechanism is equal to T_i-T_{oe}. Only the heat transfer by convective is considered.

The hydrate decomposition controlled by the heat flow is analogous with the melting moving boundary problem. At time t = 0, the reservoir is at the temperature T_i and the dissociation interface, X (t) is at x = 0. At any time t, the temperature at X (t) is equal to the equilibrium temperature with the wellbore pressure and the temperature is equal to T_i when $\infty \rightarrow x$. The derivation of the heat transfer equations of the system and its dissociation interface is shown elsewhere [Hong et al., 2003]. The analytical solution for the rate of moving of the hydrate interface as the hydrate decomposes is given by:

$$dX(t) = \lambda\sqrt{(\alpha/t)} \qquad \text{-Equation 3.2}$$

Where λ is the solution of the following equation:

$$\lambda e^{\lambda^2} erfc(\lambda) = \frac{Ste}{\sqrt{\pi}} \qquad \text{-Equation 3.3}$$

Table 3.1 Comparison of the models

Models	Energy Balance				Mass Balance		Kinetics	Solution Method	Note
	Overall		Dissociation Interface						
	Conduction	Convection	Conduction	Convection	Gas	Water			
Holder *et al.* [1982]	x				x			Numerical	Heat of dissociation from the sensible heat of the reservoir
Yousifer *et al.* [1990]					x			Analytical	
Selim and Sloan [1990]	x	x			x			Analytical	
Yousifer *et al.* [1991]					x	x	x	Numerical	- Isothermal - Kim-Bishnoi model for kinetics
Makogon [1997]	x	x			x			Analytical	Linearization and self-similar solution
Tsypkin [2000]	x	x			x	x		Analytical	
Goel *et al.* [2001]					x		x	Analytical	- Kim-Bishnoi model for kinetics - Cylindrical-shape reservoir - Gas-hydrate interface was a function of time only
Rocha *et al.* [2001]	x x	x	x x		x			Analytical Numerical	
Ji *et al.* [2001]	x	x			x			Analytical	- A temperature change because of throttling (Joule-Thompson) and adiabatic effects included in the energybalance equations - Linearization and self-similar solution
Hong *et al.* [2003]	x		x				x	Analytical	- Assumed $k \geq 1$ md and ignored the effect of fluid flow - The decomposition rate is controled by heat transfer and kinetics - Kim-Bishnoi model for kinetics - Heat of dissociation came from the sensible heat of the reservoir and the associated porous rock
Moridis *et al.* [2004]	x	x	x	x	x	x	x	Numerical	TOUGH2, EOSHYDR2
Ahmad *et al.* [2004]	x	x	x	x	x			Numerical	- Not included throttling (Joule-Thompson) effect - Finite difference method

And *Ste* is called Stefan number, which is defined as the ratio of the sensible heat of the hydrate and associate rock to the heat of decomposition:

$$Ste = \frac{\rho c_p}{\varphi \Delta H_d} \qquad \text{-Equation 3.4}$$

Where, ρ is the density of porous medium including the hydrate (kg/m^3), c_p is the heat capacity (kJ/kgK), and φ is the porosity. The parameters used in the study are shown in **Table 4.3.**

3.1.2 Decomposition Rate Controlled by Intrinsic Kinetics

At the hydrate-gas interface, the hydrate dissociation into water and gas is controlled by the kinetics of decomposition. Kim et al (1987) proposed that the hydrate decomposition rate is proportional to a driving force defined by the difference between the fugacity of methane at the three-phase equilibrium and the fugacity on methane in the bulk, and the specific decomposing hydrate surface area per unit hydrate volume (a_{dec}). Considering methane as an ideal gas, the fugacity can be simply replaced by the pressure of methane at the equilibrium pressure, p_{se}, and the pressure of the bulk gas p_g. From the mass balance around the hydrate-gas interface, the relationship between the molar rate of hydrate decomposition and the location of the interface, the analytical solution for the rate of moving of the dissociation interface is given:

$$\frac{dx}{dt} = \Psi \frac{M_H}{\rho_H} k_d \left(P_{se} - P_g\right) \qquad \text{-Equation 3.5}$$

where Ψ is the dimensionless surface roughness factor, M_H is the molecular weight of hydrate (g/mol CH_4 in hydrate), ρ_g is the pressure of methane at the solid surface (MPa), and the decomposition rate constant (k_d), defined by:

$$K_d = K_o\, e^{-E/RT} \qquad \text{-Equation 3.6}$$

Where k_o is the intrinsic rate constant for decomposition (kmol/m^2-kPa-s), E is the activation energy, and R is the gas constant.

The driving force is the pressure difference between equilibrium pressure (p_{se}) at the surface and the bulk gas pressure (p_g). Ψ is the dimensionless surface roughness factor and defined as, $\Psi = a_{dec}/\varphi a_{geo}$, where a_{dec} is the specific decomposing hydrate surface area per unit hydrate volume, and a_{geo} is the geometry surface area. For a simplified case, Ψ is equal to unity.

Clarke and Bishnoi (2001) modified the experimental apparatus of Kim et al. (1987) and obtained the activation energy similar to that of Kim et al. (1987), however, the intrinsic rate constant is approximately 10 times smaller than that reported by Kim et al. (1987). The

kinetics parameters are shown in **Table 4.4.** The parameters from Clarke and Bishnoi (2001) and Kim et al. (1987) are compared and shown in Figure 4.1 and the results are discussed below.

3.1.3 Decomposition Rate Controlled by Fluid Flow

The continuity equation of the water in the decomposed zone is given by Aziz and Settari (1979) [after Hong et al., 2003]. It is assumes that the change of the saturation of water with time in the decomposition zone is so slow that it can be ignored, and φ and ρ are constant. The derivation of the fluid flow equation is given elsewhere [Hong et al., 2003]. The analytical solution for the continuity equation for water flow and the mass balance around the dissociation interface is:

$$\frac{dX(t)}{dt} = \sqrt{\left(\left(\frac{kk_{rw}\rho_w \Delta p}{2\,\mu_w(1-F_{Hg})\phi\rho_H}\right)\left(\frac{1}{t}\right)\right)} \qquad \text{-Equation 3.7}$$

where k_{rw} is the relative permeability with respect to water, ρ_w is the density of pure water (kg/m^3), $\Delta P = P_g - P_s$ is the pressure difference between the bulk gas pressure at the interface (P_s) and the wellbore pressure (p_o), μ_w is the viscosity of water, and F_{Hg} is the mass fraction of gas in unit mass of hydrate.

3.1.4 Decomposition Rate Controlled by Gas Flow

The derivation of the decomposition rate controlled by gas is similar to those obtained from water-flow-controlled. After solving the continuity equation for the gas flow and the mass balance around the dissociation interface, one can obtain the rate of decomposition as follows:

$$\frac{dX(t)}{dt} = \sqrt{\left(\left(\frac{kk_{gw}\rho_g \Delta p}{2\,\mu_g(F_{Hg})\phi\rho_H}\right)\left(\frac{1}{t}\right)\right)} \qquad \text{-Equation 3.8}$$

Where k_{gw} is the relative permeability with respect to gas, ρ_g is the density of gas, and μ_g is the viscosity of gas. The parameters used for the fluids flow study are shown in **Table 4.5.**

3.2. Inhibitor Injection

Through injection of chemicals to the sub-sea hydrates, dissociation of the hydrate will occur. The chemical decreases the stability of the hydrate by changing the equilibrium temperature or the pressure. In the natural gas industry, alcohols (methanol) and glycols are commonly used to inhibit hydrate formation. The reason these chemicals are often used is that they exhibit some hydrogen bonding and therefore interfere with the hydrogen bonds of the water in the hydrates. Glycols are much less volatile than methanol, but glycols are usually more costly than methanol and are therefore used less often. Besides adding polar solvents, ionic solids can also be added to dissociate the hydrate. Although it may seem wise to inject an inhibitor to destabilize the hydrate zone, the effect to the marine life and the sea floor could be detrimental. Introducing something unnatural and foreign to a system can lead to problems. Corrosion of the pipelines may occur if air dissolves in the inhibitor.

Both Ramya Venkataraman and Esra Eren did some computational modeling to see a difference between methanol and ethylene glycol to determine which inhibitor would be more economically and environmentally sound. They concluded that concentrations of both methanol and ethylene glycol of greater than or equal to 20% would be needed to cause dissociation. Based on a cost analysis, they found that methanol is $0.84/gallon (USD) and ethylene glycol is $4.75/gallon (USD). To dissociate the hydrate, 3.9×10^5 kg/d or 4.1×10^5 kg/d of methanol and ethylene glycol, respectively, would need to be injected. Inhibitor injection is neither environmental nor economic and thus is not a viable hydrate recovery method.

3.3. Thermal Stimulation

Background

The Thermal stimulation method proposes the use of a source of energy to raise the reservoir temperature, thus breaking the hydrogen bonds in the hydrate to release the gas. Methods that have been suggested in the literature are: (1) injection of hot fluid such as water, steam or brine; (2) in-situ combustion and; (3) electro-magnetic heating. In situ combustion process is basically a burning front that slowly moves from an injection well to production well. Electromagnetic heating is a process, which either uses microwave or AC current to heat the reservoir. Our main concern in this study is to evaluate the feasibility of fluid injection methods. This technique has been well characterized in the laboratory for

hydrate dissociation and is traditionally used for oil and gas recovery from conventional fields.

In the literature two approaches have been suggested for realization of hot fluid injection method. One approach is a single well, cyclic thermal injection model where hot water, brine or steam can be injected into the hydrate formation. In this method, hydrates are allowed to dissociate during a "soak" period and then gas and water are produced from the same well. Another method is use of multi-well, continuous thermal injection model. Hot water or brine will be injected from one well and dissociated gas will be produced from production well.

Hydrate thermal dissociation rates were first quantified in Holder's laboratory with the work of Kamath et al. (1987) for steady-state dissociation measurement of propane and methane hydrates using hot water as the dissociation medium. They developed an empirical correlation for dissociation rate as follows:

$$M_H / \Phi_H A = 6.464 \times 10^{-4} (\Delta T)^{2.05} \qquad \text{Equation 3.9}$$

Where M_H is the steady state of hydrate dissociation (gmol/hr) Φ_H is the volume fraction of hydrate in the core, A is the surface area at the interface (cm^2), and ΔT is the temperature difference between the bulk fluid and the hydrate interface.

In subsequent research, Kamath et al. [1987], [Sira, Patil et al., 1990] proposed to combine the thermal injection technique with inhibitors such as brine, methanol and glycol. The graph below shows a correlation for gas production as a function of the temperature difference between the bulk fluid and the hydrate interface (ΔT). Selim and Sloan [1985, 1990] developed an unsteady state model for the position and temperature profile in a moving hydrate boundary. Their model can be viewed as a pseudo steady-state model after hydrate dissociation had commenced. A schematic of their model shown in **Figure 3.1,** indicates that hydrate dissociation occurs at a moving boundary X (t) which separates the un-dissociated hydrate region from the dissociated region.

Once the temperature is exceeded, the interface will move at a decreasing velocity due to the insulating effect of increasing thickness of dissociated zone. On solving for large time, they found the following simplified solution for front velocity.

$$dX / dt = \{ \alpha q_s (T_s - T_i) / k (1+ St) \}$$ - Equation 3.10

where X is the position of decomposing interface (m), T_s is the equilibrium temperature at system pressure (K), K is the thermal conductivity of the hydrate, q_s is the specified heat flux at the decomposing surface (kW/m^2), α is the thermal diffusivity (m^2/s), and $St=\lambda/(Cp(T_s-T_i)$, where λ is the heat of dissociation kJ/mol CH_4.

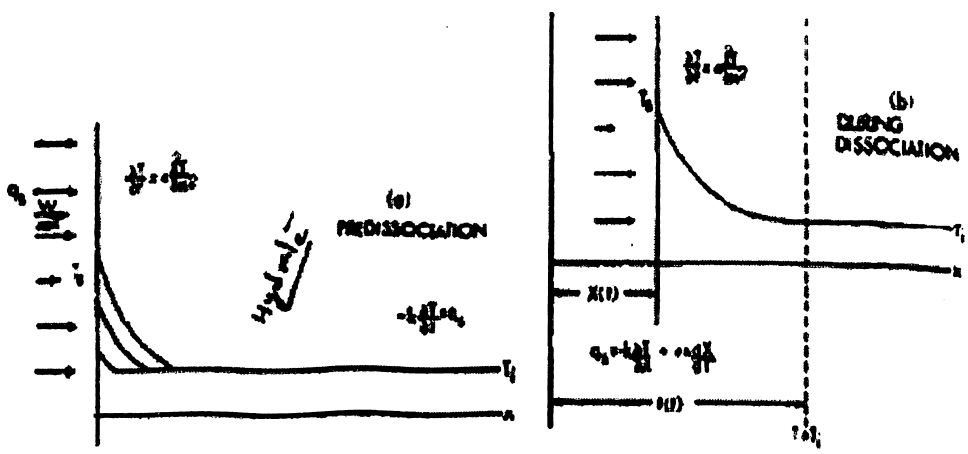

Figure 3.3 Dissociation

Approach

STEP 1: Feasibility study of thermal stimulation by determining Energy Efficiency Ratio

Energy efficiency ratio (EER) is defined as the following:

EER= Energy out put from hydrate / Energy input dissociate to hydrate

Where, energy input to dissociate hydrate includes sensible energy to increase the reservoir temperature, to the dissociation temperature and latent heat of dissociation of hydrate. Energy output is the energy produced upon combustion of natural gas.

Estimate indicates that the energy efficiency ratio of ~13 which is favorable condition as a recovery method. Supplied goes instantaneously to heat the reservoir temperature and no heat loss is accounted in overburden/under burden heating and transmission lines. Both the assumptions are very unrealistic therefore further energy analysis is carried out to determine the feasibility.

STEP 2: Selection of thermal stimulation method

Since preliminary energy efficiency of thermal stimulation is good for recovery, it is to determine how thermal energy can be provided to the reservoir. It is considered the following options for thermal stimulation method: (1) steam injection; (2) hot water injection; (3) hot brine injection; (4) methanol/glycol injection; (5) in situ combustion; (6) geo-thermal heating; and (7) addition of compressed CO_2. Each of the above mentioned methods has their own merits and disadvantages. In steam injection, heat loss in the well bore and reservoir is very high especially for thinner hydrate zone. Steam also reacts with clay and swells them which will reduce the permeability [Faure, 1998]. Another disadvantage associated with steam injection is that it will increase the water vapor in the recovered gas. Use of glycol/methanol is governed by economics because large quantity of these expensive chemicals will be required. Brine also causes most reduction in dissociation temperature. Also as a consequence, heat of dissociation is lower at lower dissociation temperatures and therefore heat losses in pipelines are lower for brine. Geothermal heating is discarded because only at certain location are these hot reservoirs found. Even if it is present, arrays of wells need to be drilled in geothermal aquifers and sediments just below the hydrate region. Gas near the circulating hot brine will dissociate, therefore additional production wells need to be drilled which will make it very expensive process. In situ combustion process is eliminated as typically 80% of the heat generated upon combustion is wasted in heating of reservoir rock

STEP 3: Selection of injection scheme

As shown above, hot brine seems to be the best injection fluid as a thermal stimulation medium. It is to determine the optimal injection scheme. Typically the following injection schemes are used for conventional oil and gas recovery: (1) cyclic injection; (2) continuous injection; and (3) recirculation of hot brine.

Though cyclic injection has the advantage of lower heat loss in pipelines and presence of heated zone near production well, it is discarded because of the periodic nature of production, and operating time delays bringing the well to production after injection phase. Shut in period can also cause refreezing of the dissociated gas during injection.

Brine recirculation is eliminated as it can heat only limited zone and a special pump is required to bring back the hot brine. Also due to very low thermal diffusivity, it is extremely inefficient process.

Continuous injection of brine has the disadvantage because the dissociation front is far from the production well and it is also limited by pore fluid pressure rise upon dissociation. However, due to continuous production of gas and very low formation depth makes it a comparatively better option among the above mentioned injection scheme.

STEP 4: Determination of well configuration and cost estimation of brine injection

We chose continuous injection for the dissociation of hydrate due to the continuous nature of production scheme. Since we are just below the sea floor, it's not possible to inject at higher pressures due to fracturing limitation. Therefore, first we calculated the fracturing pressure using the Hubbert and Willis method [Bourgoyne, Chenevert et al., 1991] mentioned below.

$$P_{ff} = (\sigma_{ob} + 2p_f) / 3 \qquad \text{-Equation 3.11}$$

where P_{ff} is the fracture pressure, P_f is the pore fluid pressure, and σ_{ob} is the overburden stress.

Using the property data for site Nag-01, it is estimated that our fracturing pressure is 9 MPa. Therefore pressure at the injection well is kept at 9 MPa and pressure at the production well is kept just below the 8 MPa. Next objective was to determine the optimal well spacing we can keep. Typically in industry, 2-5 acre well spacing design and 1 foot well bore diameter is chosen [White and Moss, 1983]. Using the standard reservoir engineering techniques [Economides and Nolte, 2000], calculated the injection rate using following formula.

$$q = (P_w - P_{wf}) (2\Pi k_h / (\mu \ln (r/ rw))) \qquad \text{-Equation 3.12}$$

Where q is the fluid injection rate, P_w is the injection pressure, P_{wf} is the wellbore pressure (8MPa), h is the thickness of the gas hydrate zone (m), r is the well spacing, and r_w is the wellbore diameter.

Once calculating the injection rate for particular well spacing (r), we calculated the rate of dissociation by assuming that upon injection, all the pore fluid is instantaneously mixed and comes at dissociation temperature. Rate of front movement is determined by locating the temperature front which lags behind the injection front by factor R which can be determined using following formula [Elsworth, 2004].

$$R = (\rho_f CP_f \varphi + \rho_r CP_r (1- \varphi) / (\rho_f CP_f \varphi)) \qquad \text{-Equation 3.13}$$

where ρ is the density of fluid, CP_f is the fluid heat capacity, CP_r is the rock heat capacity, and φ is the porosity of the medium.

After calculating the above values for a reservoir, the applicability of the thermal stimulation technique is assessed based on the economics and environmental aspects of production and its feasibility.

CHAPTER 4

CASE STUDY

4.1 History and Well data

Hydrate Ridge is 25 km long and 15 km wide ridge in the Cascadia accretionary complex. It is characterized by a northern ridge having a water depth of ~600 m and a southern peak with a depth of ~800 m. Hydrate Ridge appears to be capped by hydrate as indicated by a strong bottom-simulating reflector (BSR). In the present study our focus is to recover the gas hydrate from southern Hydrate Ridge. During Nag-01, nine sites have been drilled and cored to determine the concentration and distribution of gas hydrates. Lithology at all the sites is similar, with abundant turbidities, some debris flows and several notable ash layers. A brief summary of the findings is shown in **Table 4.1** below.

Table 4.1 Reservoir Site Assessment of Hydrate Ridge.

Region	Sites	Thickness (mbsf)	% gas saturation*	Gas volume 10^6 m3 /km2
Flank	1244,1245	45-120	3-5%	640
	1246,1247	15-115	2-4%	640
Southern Summit	1248	1-125	5-7%	805
	1249	1-30 30-90	20-40% 5-10%	965 515
Slope Basin	1250	10-110	1-3%	215
	1251,1252	30-180	1%	320

It is assumed that sediment porosity (65%) Assuming that one unit volume of hydrate will yield 164 unit volume of gas. * Saturation value chosen is average value of all the estimation methods.

The above table does not take any available free gas into consideration, thus it was not part of this study. From the above table, it is evident that gas hydrate concentration is significantly greater beneath the summit as compared with other region. Therefore, focus will be first on physical property estimation and optimal recovery methods from site NAG-01.

4.2 Properties

Permeability: Site Nag-01, spanning 300 m by 500 m, and 778 m below seafloor, is composed of clay and silty clay. This corresponds to a typical permeability of 10 md. Permeability was also estimated from capillary models [Kleinberg, Flaum et al., 2003] and is found to be 20md for 4 micrometer particle size.

Density: Wet bulk density of the samples was measured in the range from 0.35 to 7.5 g/cc. The sample shows high variability in porosity ranging from 10% to 70% and the values are negatively correlated with sample density. From this correlation, the maximum density at zero porosity was estimated to be 810kg/m^3.

Porosity: On a macroscopic scale the fabric varies from highly porous with soupy and mousse like textures. Leg Nag-01 observations clearly indicate that hydrate is present in lenses and nodules.

Pore Fluid Concentration: Pore fluid recovered from the upper 20 mbsf show pronounced enrichment in dissolved chloride concentration. The highest chloride concentration measured is 1368 mM in a sample collected. The degassing experiment document that methane concentration range from 200 to 6000 mM well above saturation value at in situ temperature(4.5 °C-9 °C) and pressure (7.9 MPa). Gamma density logs show some layers having density slightly lower than 1000kg/m^3, which indicate this layer to be pure gas hydrates. In addition a low density spike (750kg/m^3) in an 8 cm thick gas hydrate layer reveals the evidence of free gas within hydrate. Relatively high concentrations of propane and higher hydrocarbons at the start of core degassing also suggest the presence of free gas.

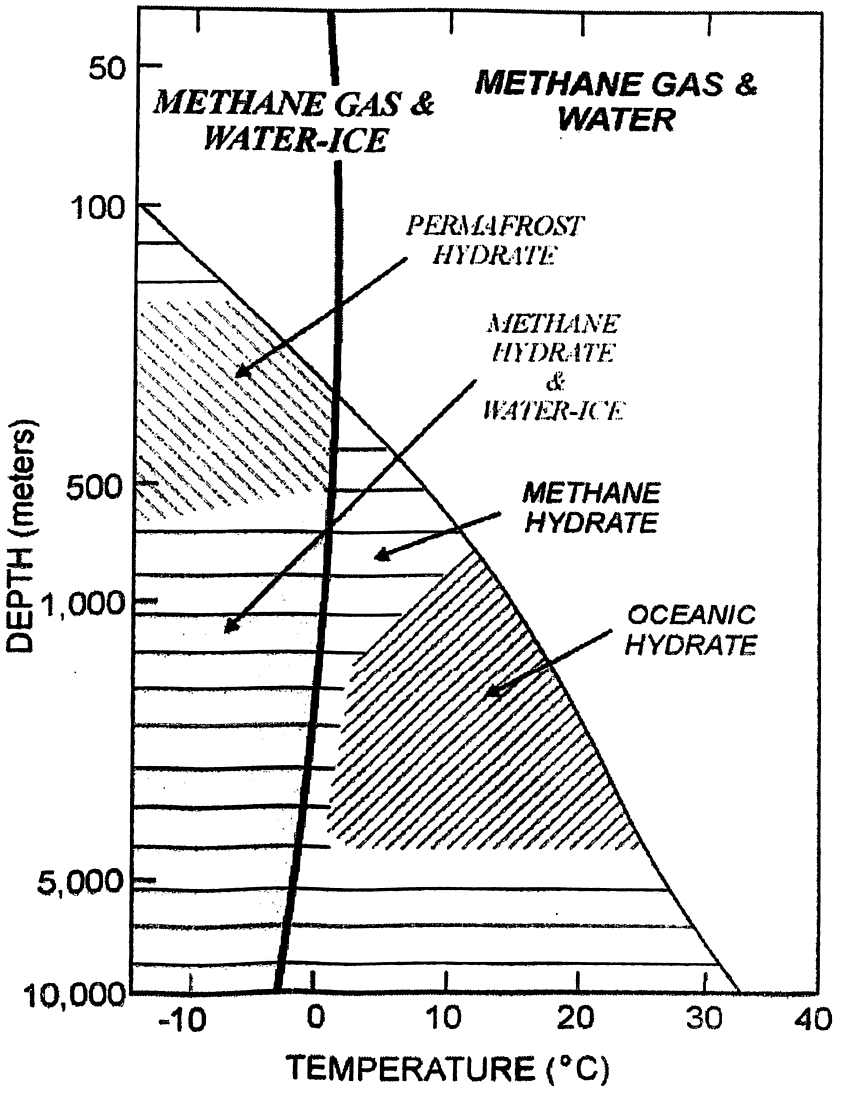

Phase Equilibrium Diagram: Since it is extremely difficult to predict the phase behavior in porous sediments, a simplified phase diagram shown left will be used for the design calculation. A brief summary of useful physical properties is mentioned in **Figure 4.1** below, and will be used for the design calculation. A brief summary of useful physical properties is mentioned in the **Table 4.2** below.

Figure 4.1 Phase Diagram showing phase behavior in porous sediments.

Source: Kvenvolden, 1999.

Table 4.2: Summary of physical properties of sediments in Hydrate Ridge.

Source: Compilation of authors listed in Works Cited Page.

Density of porous medium (ρ_r)	2675 kg/m3	Thermal conductivity of rock (Kr)	1.5 W/m k
Density of methane hydrate(ρ_h)	914.7 kg/m3	Thermal conductivity of hydrate (Kh)	0.5 W/m k
Density of methane gas(ρ_g)	80 kg/m3	Thermal conductivity of gas (Kg)	0.031 W/m k
Specific heat of rock (Cr)	0.837kJ/kg K	Thermal conductivity of water (Kw)	0.6 W/m k
Specific heat of hydrate (Ch)	1.6 kJ/kg K	Permeability (k)	10 md
Specific heat of methane gas (Cg)	2.09 kJ/kg K	Heat of dissociation (ΔHd)	13.52-0.0042 T*i* kJ/mol gas

Table 4.3 Properties of medium, pure methane hydrate, water and gas.

Parameters	Medium	Pure Methane hydrate	Water	Gas
Density*(kg/m^3)*	2675	914.7	1000	27.6
Heat capacity*(kJ/kg-K)*	0.837	1.6		
Thermal conductivity(k)*(W/m-k)*	1.5	0.5		
Heat of decomposition*(kJ/kg)*	---	477		
Thermal diffusivity*(m^2/s)*	3.562×10^{-7}	2.293×10^{5}		
Properties of methane hydrate in the medium - Density - Thermal conductivity - Heat capacity	$\rho = \rho_H \phi + \rho_R (1-\phi)$ $k_c = k_{cH} \phi + k_{cR}(1-\phi)$ $C_p = \{C_{pH} \phi + C_{pR}(1-\phi)\}/\rho$			

Table 4.4 Parameters used in the kinetics study.

Parameters	Kim et al.(1987)	Clarke and Bishoni (2001)
Δ E/R (k)	9400	9752.7
k_o *(kmol/m^2-kpa-s)*	1.24×10^5	3.6×10^4
Surface roughness	1	
MW_H(gmol CH_4 in hydrate)	119.5	

Table 4.5 Parameters used in the fluid flow study.

Parameters	Values
Permeability, k *(md)*	10
Relative permeability with water, k_{rw}	0.1
Relative permeability with gas , k_{rg}	0.5
Porosity	0.6
Viscosity of water, μ_w *(cp)*	1
Viscosity of gas, μ_g *(cp)*	0.02
Mass fraction of gas in unit mass of hydrate, F_{Hg} (kg CH_4 /kg Hydrate)	0.1339

Table 4.6 Temperatures and pressures used in the models.

Parameters	Values
Initial Temperature,T_i (K)	284
Temperature of the front surface, T_s (K)	282
Well bore pressure, P_o (MPa)	2.67
Bulk gas pressure, P_g (MPa)	4.0
Equilibrium temperature at well bore pressure, T_{oe} (K)	274
Equilibrium pressure of inter phase temperature, P_{se}	7.1
Driving force for heat transfer equations (eq. 5.4)	$T_i - T_{oe}$
Driving force for kinetic equations (eq.5.5)	$P_{se} - p_g$
Driving force for fluids flow equations (eqs. 5.7 and 5.8)	$P_g - P_o$

Depressurization:

1. $P_{se} = 10^{-6} \exp(49.3185-(9459/T_s))$

   Ts = 282 K

   Pse = 10^{-6} exp (49.3185-(9459/282)) = 7.1 MPa

Decomposition rate controlled by heat flow:

2. $dX(t)/dt = \lambda\sqrt{(\alpha/t)}$

   Sample Calculation:

   At time (t) = 1

   $$dX(t)/dt = \lambda\sqrt{\frac{\alpha}{t}} = 0.202x\ \sqrt{(0.5/1)} = 0.1428$$

   at time (t) = 2 ,dX(t) / dt = 0.101

3. $\lambda e^{\lambda^2} erfc(\lambda) = \frac{Ste}{\sqrt{\pi}}$

4. $erfc(X) = 1 - \frac{2X}{\sqrt{\pi}}\left\{\frac{1-X^2}{1!.3} + \frac{X^4}{2!.5} - \frac{X^6}{3!.7} + \ldots\ldots\right\}$

   $\lambda = 0.202$

5. Ste = $\frac{\rho Cp(Ti-Toe)}{\rho H\Phi\,\Delta H}$

Where, ρ is the density of porous medium including the hydrate (kg/m^3) = 2675

c_p is the heat capacity (kJ/kgK) = 1.6

Φ is the porosity = 0.6

= {(2675x1.6x (284-274))/ (914.7x0.6x477)} = 0.1634

Distance of front:

$$dX(t)/dt = \lambda\sqrt{\frac{\alpha}{t}}$$

Integrate the above equation with respect to (t)

$X(t) = \lambda\sqrt{\alpha}\ x\ 2\sqrt{t}$

Sample calculation:

At (t) = 1,

$X(t) = \lambda\sqrt{\alpha}\ x\ 2\sqrt{t} = 0.202x\ \sqrt{0.5}\ x\ 2\ x\ \sqrt{1} = 0.28567$

At (t) =2,

X (t) = 0.404.

Table.4.7 Calculated results of Dissociation interface by heat transfer

Decomposition rate controlled by Heat Transfer	
dX(t)/dt	Time (Years)
0.1428	1
0.1010	2
0.0824	3
0.0714	4
0.0638	5
0.0583	6
0.0539	7
0.0505	8
0.0476	9
0.0451	10

Plot no. 4.1 Rate of the dissociation interface (dx (t)/t)

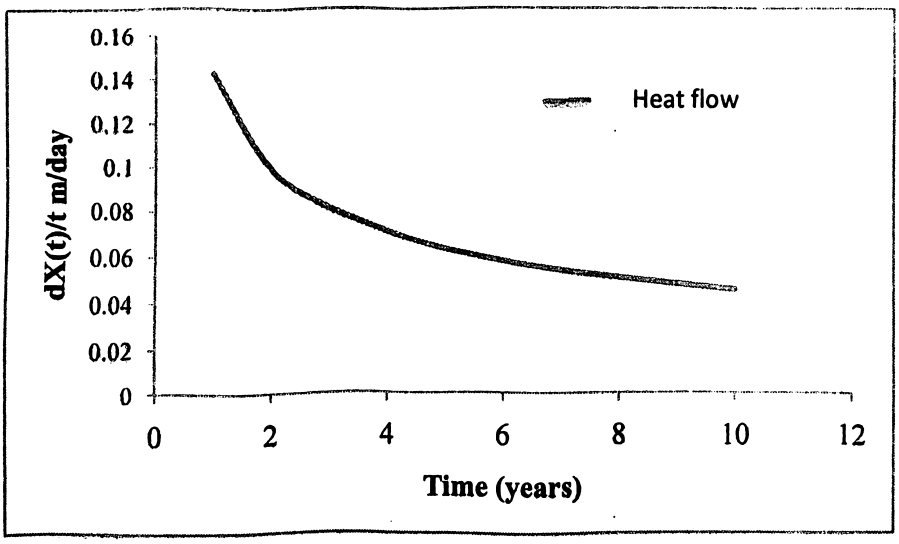

Table.4.8 Calculated results of Distance of front

Decomposition rate controlled by Heat Transfer	
X(t)	Time (Years)
0.285	1
0.404	2
0.494	3
0.571	4
0.638	5
0.699	6
0.755	7
0.808	8
0.857	9
0.903	10

Plot no. 4.2 Distance of front for heat flow

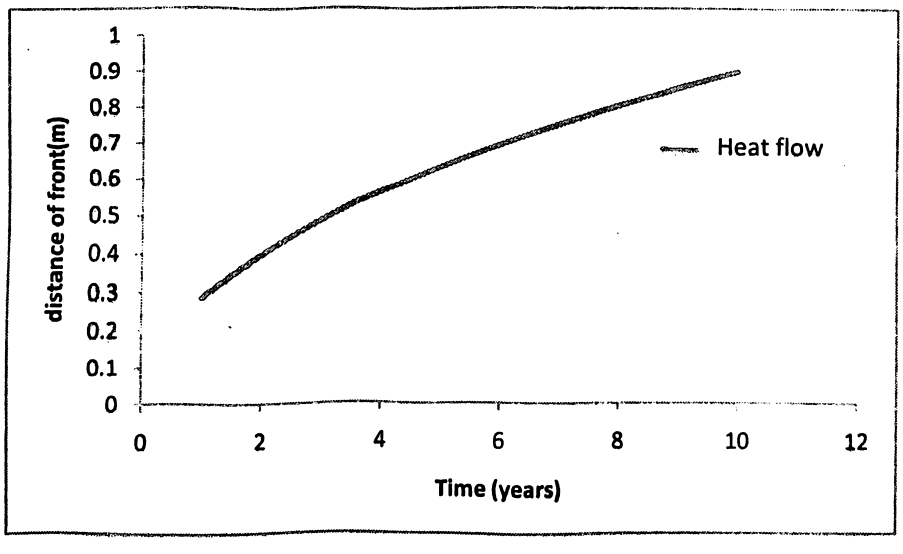

6. — —

7. $K_d = K_o\, e^{-E/RT}$

Decomposition rate controlled by fluid flow:

8. $$\frac{dX(t)}{dt} = \sqrt{\left(\left(\frac{kk_{rw}\rho_w \Delta p}{2\,\mu_w(1-F_{Hg})\phi\rho_H}\right)\left(\frac{1}{t}\right)\right)}$$

Where k_{rw} is the relative permeability with respect to water (m^2/s) =0.1

ρ_w is the density of pure water (kg/m^3) = 1000

$\Delta P=P_g-P_s$ is the pressure difference between the bulk gas pressure at the interface (P_s) and the wellbore pressure (p_o) = (4-2.67) = 1.33.

μ_w is the viscosity of water (Kg/ m.s)= 1×10^{-3}

F_{Hg} is the mass fraction of gas in unit mass of hydrate = 0.1339

Sample calculation:

At (t) = 1,

$$dX(t)/dt = \sqrt{\left[\frac{1.0\,X\,10^{-14}\,X0.1X1000X1.33}{2X10^{-3}X(1-0.1339)X0.6X914.7}X\frac{1}{t}\right]} = 1.1828 \times 10^{-6}$$

At (t) = 2, $dX(t)/dt = 8.3636 \times 10^{-7}$

Decomposition rate controlled by gas flow:

$$\frac{dX(t)}{dt} = \sqrt{\left(\left(\frac{kk_{gw}\rho_g \Delta p}{2\,\mu_g(F_{Hg})\phi\rho_H}\right)\left(\frac{1}{t}\right)\right)}$$

Where k_{gw} is the relative permeability with respect to gas = 0.5

ρ_g is the density of gas = 80 Kg/m^3

μ_g is the viscosity of gas = 0.02×10^{-3}

Sample calculations:

At (t) = 1, $dX(t)/dt = 1.3453 \times 10^{-5}$

At (t) = 2, $dX(t)/dt = 9.5127 \times 10^{-6}$

Table.4.9 Calculated results of Dissociation interface by fluid flow and gas flow

Decomposition rate controlled by fluid flow		Decomposition rate controlled by gas flow	
dX(t)/dt X 10^{-7}	Time (Years)	dX/dt X 10^{-6}	Time (Years)
0.1182	1	0.1345	1
8.3636	2	9.5127	2
6.8288	3	7.767	3
5.914	4	6.7265	4
5.2896	5	6.016	5
4.828	6	5.492	6
4.470	7	5.084	7
4.1818	8	4.75	8
3.942	9	4.484	9
3.740	10	4.2542	10

Plot no. 4.3 Rate of movement of dissociation interface for fluid flow

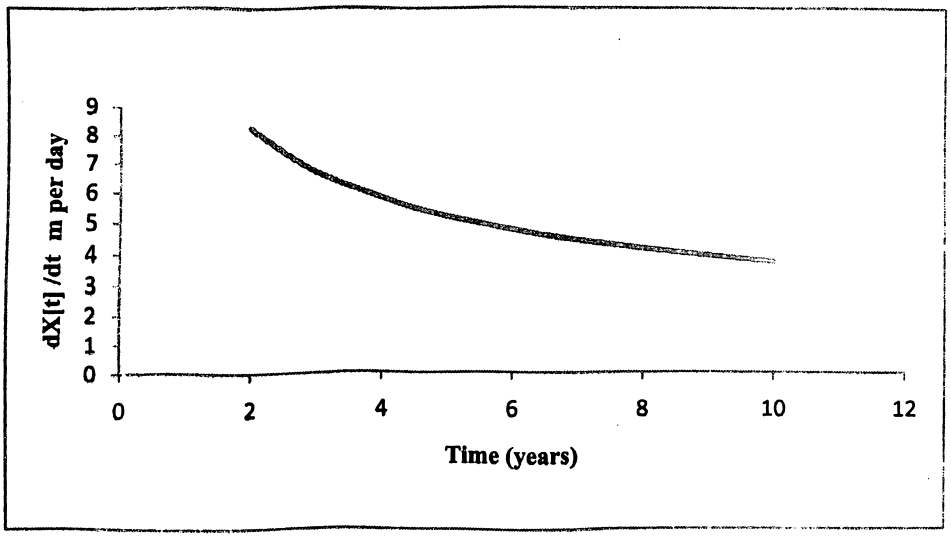

Plot no.4.4 Rate of movement of dissociation interface for Gas flow

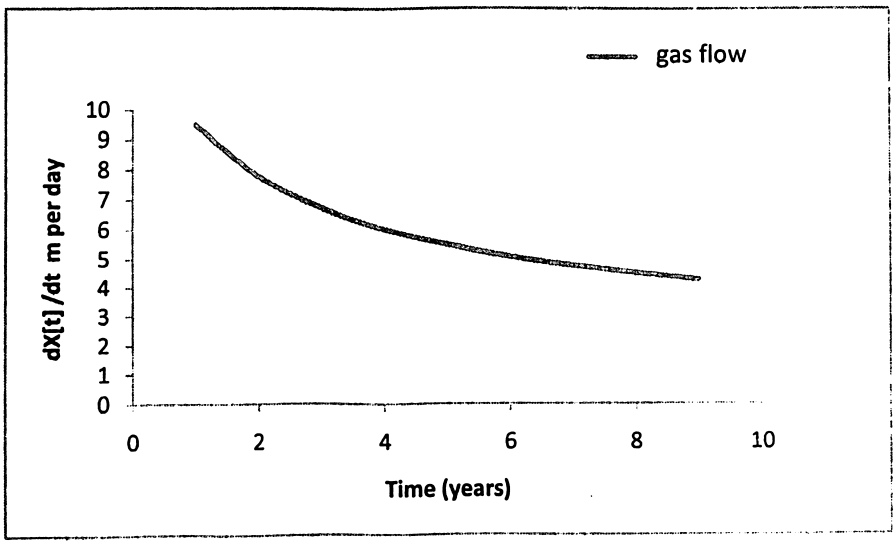

Distance of front for fluid flow:

Sample calculations:

Integrate with respect to time (t)

$$X(t) = 2 \times \sqrt{\left[\frac{1.0 \times 10^{-14} \times 0.1 \times 1000 \times 1.33}{2 \times 10^{-3} \times (1-0.1339) \times 0.6 \times 914.7}\right]} \times \sqrt{t}$$

At (t) = 1, X (t) = 2.3656×10^{-6}

At (t) = 2, X (t) = 3.345×10^{-6}

Distance of front for gas flow:

Sample calculations:

Integrate with respect to (t)

$$X(t) = 2 \times \sqrt{\left[\frac{1.0 \times 10^{-14} \times 80 \times 1.33}{2 \times 0.02 \times 10^{-3} \times 0.1339 \times 0.6 \times 914.7}\right]} \times \sqrt{t}$$

At (t) = 1, X (t) = 2.269×10^{-5}

At (t) = 2, X (t) = 3.208×10^{-5}

Table 4.10 Calculated results of Distance of front

Decomposition rate controlled by fluid flow		Decomposition rate controlled by gas flow	
Distance of Front(m) x 10^{-6}	Time(Years)	Distance of Front(m) x 10^{-5}	Time(Years)
2.365	1	2.269	1
3.345	2	3.208	2
4.097	3	3.390	3
4.731	4	4.538	4
5.289	5	5.073	5
5.794	6	5.558	6
6.258	7	6.000	7
6.690	8	6.417	8
7.096	9	6.807	9
7.480	10	7.175	10

Plot no.4.5 Distance of front for water flow

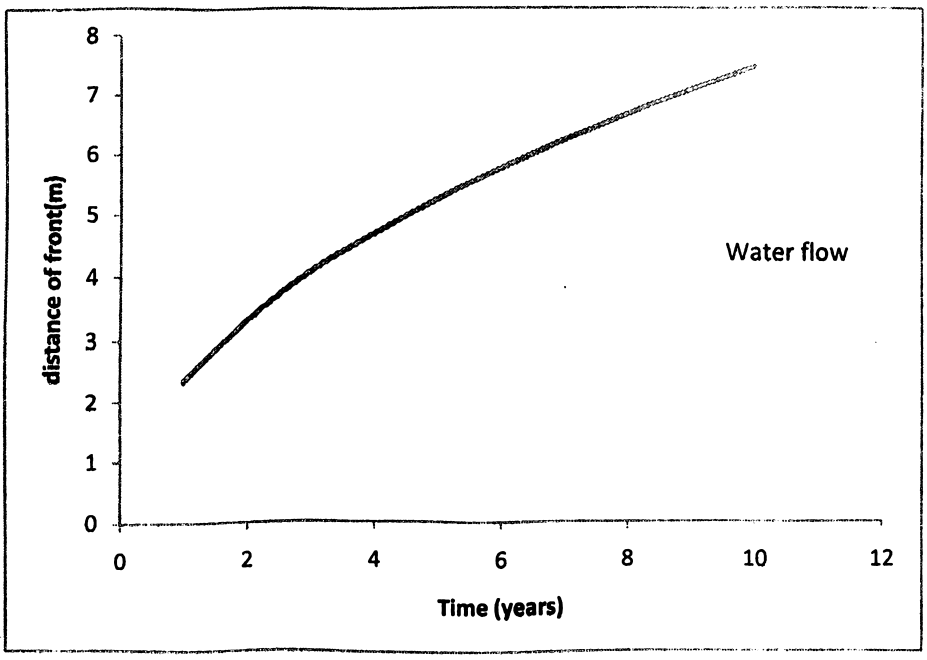

Plot no.4.6 Distance of front for Gas flow

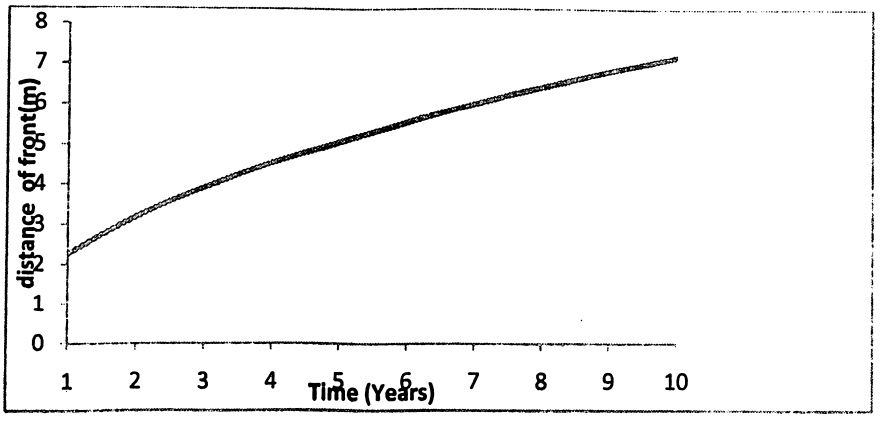

Plot no. 4. 1 – Plot no.4. 6 Comparison of the dissociation rate controlled by heat transfer, water flow and gas flow

Table 4.11 Production Rate data.

Time (Years)	Production Rate (BCF/Year)
$9.93x\ 10^{-2}$	1.4583
0.453	1.2666
1.09	1.2230
2.04	1.2171
3.30	1.317

Plot no 7. Cumulative production of well

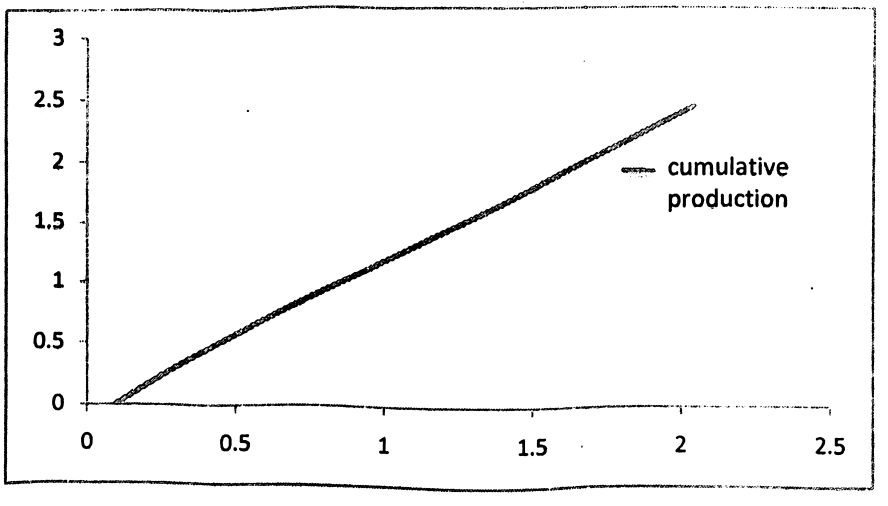

CONCLUSION

Methane hydrate presents an enormous supply of energy source and found through out the world in permafrost and continental margin of oceans. However, its optimal recovery requires that reservoir should have high hydrate saturation value. Methane that is trapped in the hydrate can be recovered and potentially used on-site. Methane hydrates can be recovered through three methods such as decompression, inhibitor injection, and thermal injection. Each method has advantages and disadvantages related to site properties and safety. Each characteristic, including the potential methods of recovery was discussed in this review.

For the hydrate ridge suggests the followings:-

1. Hydrate saturation is very low except summit region.
2. Due to very low permeability and high hydrate saturation value at summit, thermal injection method is suggested as a potential recovery method. Recovery from other sites will make this recovery method infeasible.
3. Using thermal injection method, we can produce 1-3 BCF/year
4. The production by only depressurization is not economical in this case. With the help of hot fluid injection, this would eliminate the heat transfer effect and help enhancing the kinetics of dissociation. If the heat transfer and kinetics are no longer the rate limiting steps, we can be able to meet target production rate.
5. Inhibitor injection is neither environmental nor economic and thus is not a viable hydrate recovery method.

BIBLIOGRAPHY

1. D.Nasipuri, Stereo Chemistry of organic Compounds, New age international P Ltd,2nd edition, Pg.No.156.

2. Pteitter.P, Organische molekulver bindungon, 2nd edition, chemie, In Einzeblarste llungen, vol.II, Stuttgart, 1927.

3. Hertl, E. Komer, G.H., Ber, 63B, 2446 (1930)

4. clap, leallyn B., the chemistry of coordination compounds, Ed John . c. Bailer, Jr., Network, Rein hold publishing corp., 1956.

5. Eeteloar, J.A.A, chemical constitution, second Ed, Elsevier, Pub. Co., Pg.363, 1958.

6. Robertson, Johnm, Organic Crystal and molecules, Cornelluniv, press p.g. 246, 1953.

7. Baron, Maximo, Org. chem.. Bull. 29,(2), 1957.

8. Sang- yong. Lee, Gerald D. Holder- methane hydrate potential as a future energy source, fuel processing tech, 71(2001) 181-186

9. Technical Data book, Petroleum- refining- Refining Department 6th ed. API 1997, pg-9-41 to 9-42

10. E. Arunan, definition of hydrogen bond, IISC, Aug 2005

11. Serge N. Vinogradov and Robert H. Linnell, Hydrogen bonding, Ven Norstrond Reinhold Company 1971, page 11-12,

12. Evens, An introduction to Crystal Chemistry, Cambridge University, Press, 2nd edition, 1966, page no. 248.

13. En. Yeremin, Fundamentals of Chemical thermodynamics, MIR publishes, Moscow, 1981, pg 94 to 97, 214 to 219

14. E. Dendy Sloan Jr., Fundamental Principles and applications of NGH, Nature, Vol.426, 20 Nov 2003, pg.354

15. Natural gas production from hydrate decomposition by depressurization, Chuang Ji National Energy Technology Laboratory, US Department of Energy, Morgantown, WV 26507-0880, USA. Received 10 March 2000; received in revised form 23 October 2000; accepted 24 April 2001.

16. www.elsevier.com/locate/ces

17. Advances in the Study of Gas Hydrates, Edited by Charles E. Taylor and Jonathan T. Kwan. Page no.43 and 83.

18. Natural Gas Hydrate In Oceanic and Permafrost Environments, Edited by Michael D.Max Page no.46.

19. Natural Gas Hydrates, A Guide for Engineers, by John J. Carroll.

20. Gas Hydrate Relevance to World Margin Stability and Climate change, Edited by J.-P.Henriet & J.Mienert.Geological Society Special Publication No-137.

21. Economic Geology of Natural Gas Hydrate, Coastal Systems and Continental Margins, Volume-9, Bilal U. Haq. Page no.249.

22. Down-hole combustion method for gas production from methane hydrates, Marco J. Castaldi, Yue Zhou, Tuncel M. Yegulalp, Department Earth and Environmental. Eng., Henry Krumb School of Mines, Columbia University, New York, NY, USA. Received 6 October 2005; accepted 3 March 2006.

23. Fundamental principles and applications of natural gas hydrates, E. Dendy Sloan Jr. Center for Hydrate Research, Colorado School of Mines, Golden, Colorado 80401, USA (e-mail: esloan@.mines.edu)

24. www.Sciencedirect.com

25. Strategies for Gas Production from Hydrate Accumulations Under various Geological and Reservoir conditions, George J. Moridis and Timothy S. Collett. PROCEEDINGS, TOUGH Symposium 2003 .Lawrence Berkeley National Laboratory, Berkeley, California, May 12–14, 2003.

26. Clathrate Hydrates of Natural Gases, Second edition, Revised and Expanded, E.Dendy Sloan Jr. Page no.525 and 533.